

## NUMERICAL SIMULATION OF OBSERVED LIQUEFACTION PHENOMENA FROM THE 2011 CHRISTCHURCH EVENT

Silvia BERTELLI<sup>1</sup>, Diego MANZANAL<sup>2</sup>, Susana LOPEZ-QUEROL<sup>1</sup>, Tiziana ROSSETTO<sup>1</sup>, Pablo MIRA<sup>2</sup>, Sonia GIOVINAZZI<sup>3</sup>, Rob RUITER<sup>4</sup>

**Abstract:** Soil liquefaction at the ground often cause damages to various infrastructure assets. Its consequences have been widely made evident by the performance of the Telecommunication Network Services during the 2010-2011 Canterbury Earthquake Sequence (CES) which stroke the Canterbury region in New Zealand. Despite the relevance of loss of functionality of the telecommunication system, especially during the post-event recovery phase, studies in the literature on the network performance about damages due to liquefaction are still limited. Exploring an unprecedented database of in-situ geotechnical inspections collected after the CES, this research first compares alternative empirical liquefaction-triggering models available in the literature with observation maps. Then, a soil column profile is evaluated adopting a constitutive model based on generalised plasticity ('modified Pastor-Zienkiewicz') through a Finite Element based home-developed code. The obtained results from the numerical models are finally cross-checked with the empirical analyses, the existing liquefaction investigation maps and field observations collected in the aftermath of the CES.

### Introduction

Large-scale urban infrastructure networks are highly susceptible to liquefaction. Buried lifelines failures due to floatation or differential settlements are often recorded on telecommunication, electric power, and water and wastewater systems (Maurer *et al.*, 2015; Chian *et al.* 2012, 2014). For instance, in the aftermath of 22nd February Christchurch Event (New Zealand), Telecom investigations reported many utility holes partially floated out of the ground or filled with water in areas where there was severe liquefaction. The majority of faults were recorded on the copper network in the liquefied areas (Tang *et al.*, 2014). The telecom infrastructure was robust enough and required limited maintenance procedures for its restoration compared to other systems. Nonetheless, the impact of the liquefaction on the network can still be observed from the utility holes left uplift after almost ten years since the event (Figure 1).

Regarding the Mw=6.2 Christchurch earthquake itself, the event was induced by a strike-slip rupture, centred 10 km to the southeast from the Central Business District (CBD) at 5-6 km depth. Due to its shallow depth and proximity to the CBD, very high ground motions were registered by the 33 recording stations placed around the Canterbury region. Liquefaction manifestations, including the significant sand boilings, slumpings and ground settlements observed, are one of the most extensive and severe ever reported worldwide (Taylor, 2015).

---

<sup>1</sup> EPICentre, Department of Civil, Environmental and Geomatic Engineering, University College London, London, WC1E 6BT, UK

<sup>2</sup> Department of Continuum Mechanics and Structures, ETSI Caminos, Canales y Puertos, Universidad Politecnica de Madrid, Spain

<sup>3</sup> Department of Civil and Natural Resources Engineering, University of Canterbury, Christchurch, New Zealand

<sup>4</sup> Manager Network Protection, Chorus, Christchurch, New Zealand



Figure 1. a) Liquefaction inside telecommunication ducts in a utility hole (Courtesy of Chorus Ltd) b) Uplifted utility hole in the CBD of Christchurch.

Thus, the objective of this study is to investigate the liquefaction potential of the soils in Christchurch, and it is part of broader research on liquefaction-induced damages on the telecom networks. Specifically, this study aims to compare results from state-of-practice semi-empirical models to the ones obtained from a constitutive model based on generalised plasticity ('modified Pastor-Zienkiewicz', MPZ). Geotechnical information for both the semi-empirical and numerical methods are gathered from the New Zealand Geotechnical Database (NZGD), an online repository of information developed after the 2010-2011 Canterbury Earthquake Sequence (CES).

In the following, after an overview of the geomorphological setting of Christchurch, data and state-of-practice semiempirical methodologies for the triggering assessment of liquefaction is presented. Results demonstrate that their prediction is rather casual, as they tend to overpredict the occurrence, but they can also underpredict the occurrence of liquefaction. Then, a soil column is simulated using a finite element model (GeHoMadrid), in which the aforementioned MPZ constitutive law has been implemented. The results are compared with the analysis carried out using empirical analysis. The results from the numerical analysis demonstrate that, despite the high fines content, liquefaction is likely to occur in the selected location, which is in agreement with the observations but not with the empirical ones.

### Geomorphologic background

Liquefaction is a well-recognised hazard for Christchurch (Brackley, 2012). The city is placed on the Pacific coast and surrounded by the Heathcote, Avon, and Waimakariri Rivers, which explains the shallow Ground Water Table (GWT) as well as loose, low-plasticity, poor consolidated, Holocene alluvial deposit soils. Historically, before the Christchurch Earthquake, liquefaction manifestations have occurred during the 2010 Darfield Earthquake through the city, even though less extensively. Manifestations were also recorded at the estuary of the Avon and Heathcote rivers in 1869, coastal areas from Kaiapoi northwards during the Cheviot earthquake in 1901, and Motunau earthquake in 1922 (Brackley, 2012).

The observed lateral spreading, sand boils, settlements, silt mud ejections and water ponding on the ground surface observed during the Christchurch earthquake are consistent with the geology of the area (Giovinazzi *et al.*, 2011) Indeed, the shallowest soil above which the city lies has a quite recent formation (Figure 2). The basement rock and the rocks of the volcano which form the current Bank peninsula were originated, respectively, during the Permian-Cretaceous Period and Miocene Era. Instead, the Canterbury Plain formed during the last part of the Quaternary Age through interfingering of river gravels eroded from the basement rocks of the Canterbury foothills and the South Alps with fine-grained shallow marine and coastal sediments (Brackley, 2012).

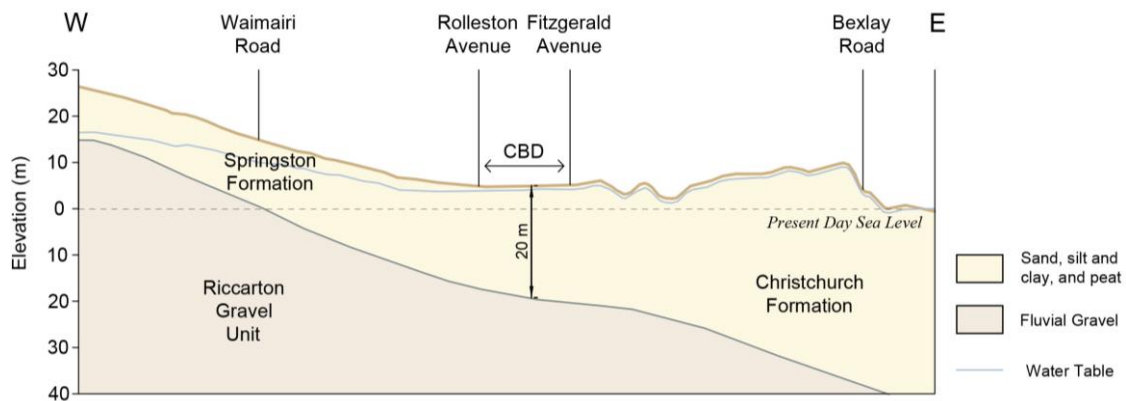


Figure 2. Schematic geologic section of Christchurch (after Brown & Weber, 1992).

In particular, the superficial soil conditions under the central business district (CBD) broadly comprise the Springston and Christchurch Formations. The first is an alluvial soil principally originated from the periodic floods of the Waimakariri River through the city. These deposits overly and Christchurch Formation marine sands which, in turn, are mixed with silt-clay estuarine and swamp deposits accumulated following the last glaciation. Below these deposits, at approximately 20m depth in the CBD, there is an older Riccarton Gravel formation deposited during the last glaciation (Figure 2). As a consequence, a substantial area of Christchurch is underlain with sand that would be highly susceptible to liquefaction (Maurer *et al.*, 2014).

Regarding the mineralogy of the superficial formations, no differences have been observed between fine and coarser particles or between marine sands of the Christchurch Formation and the fluvial sands of the Springston Formation (Taylor, 2015). Generally, the Christchurch Formation is a uniform fine quartzitic – feldspar sand with a mean diameter  $D_{50} = 0.03 - 0.14$  mm and a uniformity coefficient  $c_u = 2.3 - 6$ . The specific gravity is 2.65, and the minimum and the maximum mean void ratio are 0.62 and 1.29, respectively. Instead, the Springston Formation is composed mainly by silty sands and sandy silts (FC 13 –58 %), with  $D_{50}$  between 0.04 and 0.29 mm, and  $c_u$  between 1.9 and 5.18.

The geologic process is also mirrored in the current water flow regime (Figure 2). The GWT lies several meters or more below the surface on the west areas on the Canterbury plain, and it rises to the surface closer to the coast. This fluctuation is evident in Christchurch itself where the GWT is at approximately 2-3 m depth in the western suburbs and 0-2 m in the eastern ones (Maurer *et al.*, 2014). Nonetheless, the GWT fluctuates seasonally throughout the year and from year to year over a meter. As a result, these hydraulic and geologic features might increase the potential susceptibility of Christchurch soils to undergo liquefaction during major seismic events, as sandy soils are required to be saturated to liquefy.

## Semi-empirical analysis

### Data

Unprecedented levels of liquefaction were surveyed across a wide area in the suburbs north to south of the city, and northeast along the River Avon after the Christchurch Earthquake. For the current research, a property and road observation severity maps developed through on-foot surveys (NZGD, 2013) is adopted as a reference. This source classifies the observations as none, minor, moderate, severe, moderate-to-severe, very severe based on the evidence and quantity of ejected material as well as the lateral displacement which was visible at the surface.

As far as the geotechnical data is concerned, the primary methods of soil investigation performed after the event are the CPT and SPT site tests. The NZGD makes publically available, respectively, more than 30,000 CPT and approximately 18,000 SPT tests. Through this dataset, 58 high-quality records located across the entire municipal territory are selected for comparison of different liquefaction potential methodologies as indicated in the next subparagraph. These soundings are chosen based on the assessment of their location as susceptible to liquefaction, the availability of both soundings at the same location, termination depth over 10 m, proximity to ground motions recording stations, and availability of piezometer readings.

### Methodology

The state-of-practice procedure for the triggering assessment of liquefaction potential is mostly based on a semi-empirical method first presented in the early 1970s (Seed & Idriss, 1971). Since then, several variations have been proposed based on back-analyses of case studies (Youd & Idriss, 2001). By way of illustration, correlations for different field tests (i.e. Standard Penetration Test, SPT, Cone Penetration Test, CPT, and shear wave velocity measurements,  $V_s$ ) have been introduced to provide a low-cost in-situ alternative for evaluating the soil resistance to liquefaction.

In order to estimate the correspondent Factor of Safety against liquefaction for all the selected CPT soundings, 13 different models based on the semi-empirical relationships reported by Youd & Idriss (2001), Moss *et al.* (2006), Idriss & Boulanger (2008), Boulanger & Idriss (2014) are adopted as described in Bertelli *et al.* (2019). For the application of these relationships, soil unit weights are presumed to be 17 kN/m<sup>3</sup> above the GWT, and 19.5 kN/m<sup>3</sup> below the GWT (Wotherspoon *et al.*, 2014). The PGA at each CPT site is extrapolated from a conditional PGA isoseismal map for liquefaction assessment retrieved from the NZGD (2015). For the estimation of Liquefaction Potential Index (LPI) values (Iwasaki *et al.*, 1978) layers are considered to be potentially liquefiable if the soil behaviour type index ( $I_c$ ) is less than 2.6 (Robertson & Wride, 1998). A correlation is then established between the calculated LPI values and the observed liquefaction manifestations reported in the observation maps previously mentioned. In particular, the prediction of liquefaction occurrence is reduced to a binary system according to the Iwasaki methodology (i.e. if  $LPI \geq 5$ , liquefaction manifestations are expected at the investigated site).

### Results

The observations' map and the obtained LPI values are reinterpreted, as indicated in Bertelli *et al.* (2019). Each observation site is considered either as "No Liquefaction" or "Liquefaction"; "none" and "marginal" classes are mapped as negative results of occurrence, whereas the other types as positive. Then, each observation-calculated combination case is arranged according to a confusion matrix approach as True-Positive (TP), True-Negatives (TN), False-Positive (FP), and False-Negative (FN). Based on this confusion matrix classification, exploratory spatial analysis is carried out to evaluate the overall LPI performance of the tested methods, as shown in Figure 3.

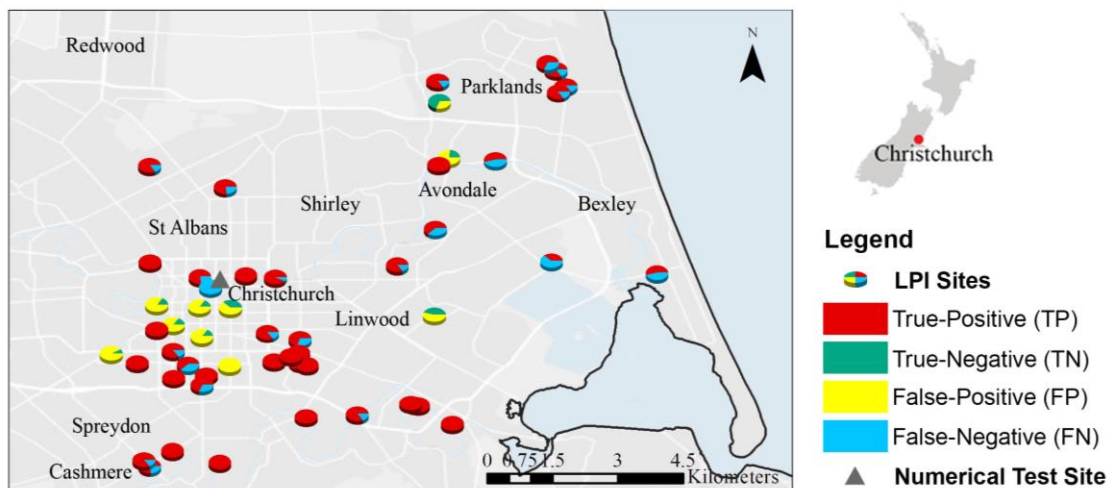


Figure 3. Comparison of observation liquefaction data with 7 LPI prediction models: True-Positive (TP), True-Negative (TN), False-Positive (FP), False-Negative (FN).

As can be seen in Figure 3, the exploratory spatial analysis results in a general over-prediction of the semi-empirical models. The pie-charts adopted for symbolising the cumulative results from the thirteen different methodologies at each test location are predominantly "yellow" (False-positive) in the western suburbs of Christchurch. This inconsistency between the predictions and observations is might due to the geomorphological features of this area. The increasing mix of sand, silt and gravel in these soil profiles would have misled the calculation of  $I_c$  factors, which resulted in higher LPI values and lead to an overprediction of liquefaction manifestations.

A remarkable aspect of these semi-empirical models is that they may also under-estimate the potential of liquefaction occurrence. For instance, none of these models has provided correct

predictions for 144 Kilmore Street Location. This discrepancy could be attributed to a higher GWT level compare to other areas where severe liquefaction was observed and correctly predicted. However, the rather contradictory result for 144 Kilmore Street Site might also depend on the misleading procedure used to classify the soil, which results in clay-like material instead of silty-sand due to the high level of fines content.

**Numerical Analysis**

*Data*

Laboratory tests performed on a soil column corresponding to 144 Kilmore Street Site (-43.5264, 172.6400) can provide further insights (Taylor, 2015). This location has the potential for both liquefaction and lateral spreading, as it is situated immediately north of the Avon River, where flood overbank deposits have accumulated. This street was severely affected by liquefaction-induced ground deformation after the Christchurch event. Materials of the soil column at this location consist of loose to medium dense grey finely interbedded silty fine sands and sandy silts (reworked flood over-bank deposits), with non-plastic fines contents of 120 mm between 15 and 50% in the upper 8 m. Then, medium-dense and then dense brown clean medium sands (marine beach/dune sands) are present up to 22 m depth.

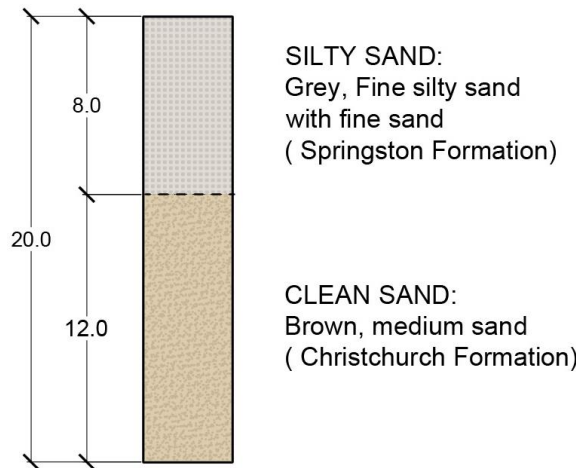


Figure 4. Model constants for the two different soils for the MPZ constitutive model.

As indicated by the recordings obtained from PEER Ground motion Database (Ancheta *et al.*, 2013) the highest recorded Peak Ground Acceleration (PGA) was 0.32g at Christchurch Resthaven REHS (-43.5015, 172.021), the closest recording station from 144 Kilmore Street (see Figure 5).

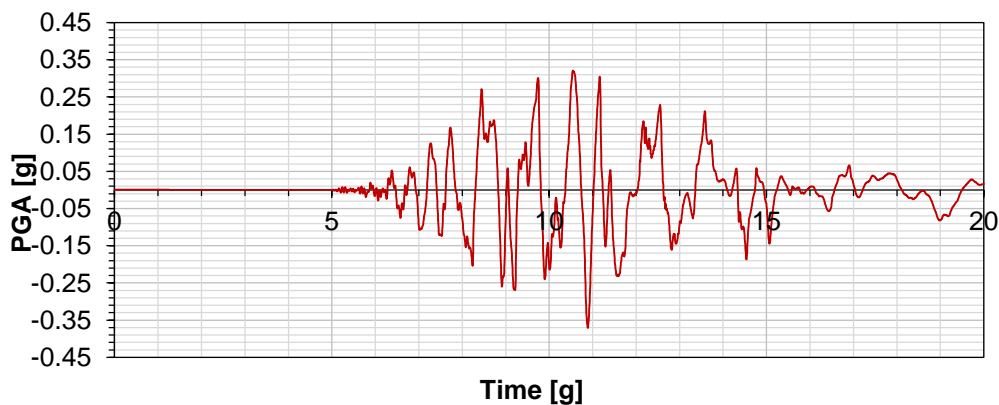


Figure 5. Horizontal PGA north component recording at REHS location, the closest recording station to 144 Kilmore Street during the 2011 Christchurch Event.

*Methodology*

In order to assess the liquefaction potential of the selected location, a two-dimensional finite element mesh is created (Fig.6). Both lateral boundaries of the soil column are assumed as impermeable. Pore pressures are assumed to be zero at the surface of the layer. The finite element model consists of 20 stabilised four-node quadrilateral elements, where bilinear shape functions are used both for displacements and pressures. The lateral nodes have repeated boundary conditions, where the displacement of a right-hand side node are equals to the corresponding left-hand side node. Time stepping adopted was 0.02s (Haigh et al 2005).

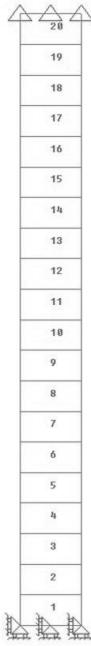


Figure 6. Finite element mesh for soil layer of 20m at 144 Kilmore Street Location.

Parameter		Silty Sand	Clean Sand
Elasticity	$G_{eso}$	125	125
	$K_{evo}$	167	167
Critical state	$M$	1.38	1.38
	$\Gamma$	0.952	0.975
	$\lambda$	0.085	0.060
Plastic flow	$\zeta$	0.45	0.47
	$d_0$	0.88	0.88
	$m$	3.5	3.5
	$h_1/h_2$	1.31 / 0.85	1.31 / 0.85
Plastic modulus	$H'_0$	125	125
	$\beta'_0$	1.9	1.9
	$\beta$	1.8	1.8
	$H_{v0}$	175	175
	$\beta_v$	1.5	1.5

Table 1. Model constants for the MPZ constitutive model.

Regarding the soil column materials, the 20 m of the soil layer is modelled as a column divided in an upper silty-sand layer of 8m and a lower clean sand layer of 12 m, which correspond to the Springston and Christchurch Formations. In particular, the upper eight elements of the soil column are assumed to be silty sand at loose state ( $e_0 = 1.031 - Dr = 23\%$ ) with 17% of fines contents. The lower 12 elements clean sand at medium dense state ( $e_0 = 0.825 - DR = 46\%$ ) associated with Christchurch formation with fines contents less than 1%.

The constitutive behaviour of this soil has been modelled using the generalised plasticity critical state-based model MPZ proposed by Manzanal *et al.* (2006). MPZ model extends the Generalised Plasticity constitutive equation in order to reproduce stress-strain behaviour of granular soils with a single set of intrinsic model constant for different densities, confining pressures and saturation conditions. In particular, it is developed assuming that the material is isotropic, and therefore, it is formulated in terms of the three invariants of the effective stress tensor  $p$ ,  $q$  and  $\theta$  together with the work conjugate strain invariants  $\epsilon_v$  and  $\epsilon_s$ . Thus, the material parameters used for representing both silty-sand and clean sand are reported in Table1. The effect of the fine contents was introduced on the critical state parameters, adopting a single set for both formations with accurate results in representing the laboratory tests.

Then, the 20 m soil column is subjected to the North component accelerogram for the Christchurch earthquake measured at REHS recording station reported in the previous Figure 5.

### Results

Figure 7 presents the evolution of excess of pressure along the soil column for different times (2.0s, 5.0s and 10.0s) in conjunction with effective vertical stress.

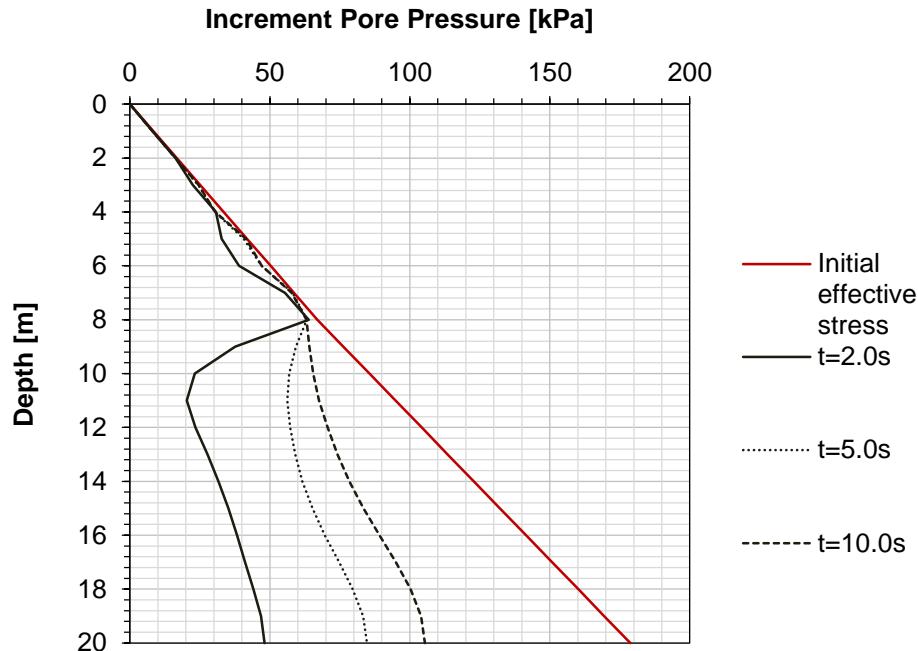


Figure 7. Excess pore pressure: loose upper layer and medium dense lower layer.

As it can be seen, the MPZ model predicts the occurrence of liquefaction for the whole 8 m layer within the first two seconds, whereas the increment of excess pore pressures is more gradual and do not reach liquefaction for the deeper layer. These results obtained through a more robust and advanced method are supported by the observation of severe liquefaction manifestations recorded after the Christchurch event and are in agreement with most of the studied empirical models.

### Conclusion

This paper summarised the application of a number of well known and extended empirical methods for the liquefaction potential to the area of Christchurch, as well as presenting and advanced numerical analysis. In particular, the Modified Pastor Zienkiewicz generalised plasticity model is adopted, which includes the fines content as a variable to define the location of the critical state line. It can be seen how the empirical methods tend to overpredict the liquefaction occurrence, while the numerical analysis properly concludes the liquefaction in the selected location, which is in fair agreement with the site observations.

Although proven as more accurate, the numerical models require more detailed site-specific geotechnical data and laboratory tests to be calibrated, and as such are less appropriate for regional-scale analysis (López-Querol & Blázquez, 2006).

### Acknowledgements

The authors are grateful to Dr Myrto Papaspiliou from Willis Research Network, Dr Liam Wotherspoon from QuakeCoRE – University of Auckland, and the Civil and Environmental and Geotechnical Engineering Department (University College London), which have also supported this research project through the Urban Sustainability and Resilience Doctoral Training School. The authors also gratefully acknowledge the financial support for research granted by the Spanish Ministry of Education under the mobility program “José Castillejo”.

## References

- Ancheta, T.D., Darragh, R.B., Stewart, J.P., Seyhan, E., Silva, W.J., Chiou, B.S., Wooddell, K.E., Graves, R.W., Kottke, A.R., Boore, D.M. and Kishida, T. (2013). Peer NGA-West2 database.
- Bertelli, S., López-Querol, S., Ruiter, R., Rossetto, T., Giovinazzi, S. & Wotherspoon, L. (2019). Comparison of Different Liquefaction Assessment Methods with Data from the 2010-2011 Canterbury Earthquake Sequence. *7th International Conference on Earthquake Geotechnical Engineering (VII ICEGE)*.
- Boulanger, R.W. & Idriss, I.M. (2014). *CPT and SPT based liquefaction triggering procedures*. Report No. UCD/CGM-14/01. Center for Geotechnical Modeling, University of California Davis, California.
- Brackley, H.L. (2012). Review of liquefaction hazard information in eastern Canterbury, including Christchurch City and parts of Selwyn, Waimakariri and Hurunui Districts, *GNS Science Consultancy Report 2012/218*.
- Brown, L. & Weeber, J. (1992). *Geology of the Christchurch urban area*. Institute of Geological and Nuclear Sciences, Lower Hutt, New Zealand.
- Chian, S.C. & Madabhushi, S.P.G., (2012), Effect of soil conditions on uplift of underground structures in liquefied soil, *Journal of Earthquake and Tsunami*, DOI: 10.1142/S1793431112001334.
- Chian, S., Tokimatsu, K., and Madabhushi, S., (2014), Soil Liquefaction–Induced Uplift of Underground Structures: Physical and Numerical Modeling, *ASCE Journal of Geotech. Geoenviron. Eng.*, 140(10), 04014057.
- Fernandez Merodo, J.A., Pastor, M., Mira, P., Tonni, L., Herreros, M.I., Gonzalez, E., Tamagnini, R. (2004). Modelling of diffuse failure mechanisms of catastrophic landslides. *Computer Methods in Applied Mechanics and Engineering*; **193**: 2911-2939.
- Giovinazzi, S., Wilson, T., Davis, C., Bristow, D., Gallagher, M., Schofield, A., Villemure, M., Eidinger, J., Tang, A. (2011). Lifelines Performance and management following the 22 February 2011 Christchurch Earthquake, New Zealand: Highlights of Resilience. *Bulletin of the New Zealand Society for Earthquake Engineering*. 44 (4), pp.402-417.
- Haigh, S.K., Ghosh, B. and Madabhushi, S.P.G., (2005), The effect of time step discretisation on dynamic finite element analysis. *Canadian Geotechnical Journal*, Vol. 42(3), pp 957-963.
- Idriss, I. & Boulanger, R. (2008). *Soil Liquefaction during Earthquakes*. Monograph Series: Earthquake Engineering Research Institute, Oakland, California.
- Iwasaki, T., Tatsuoaka, F., Tokida, K., & Yasuda, S. (1978). *A practical method for assessing soil liquefaction potential based on case studies at various sites in Japan*. Proc., 2nd Int. Conference on microzonation, National Science Foundation, Washington, D.C.
- López-Querol, S. & Blázquez, R. (2006). Liquefaction and cyclic mobility model for saturated granular media. *International journal for numerical and analytical methods in geomechanics*, 30(5).
- Manzanal, D., Fernández Merodo, J.A., Pastor, M. (2006). Generalized Plasticity Theory Revisited: New advances and applications. In proceeding of *17<sup>th</sup> European Young Geotechnical Engineer's Conference Zagreb*, Szavits-Nossan V Ed. Zagreb, Croatia, 238-246.
- Maurer, B.W., Green, R.A., Cubrinovski, M. & Bradley, B.A. (2014). Evaluation of the liquefaction potential index for assessing liquefaction hazard in Christchurch, New Zealand. *Journal of Geotechnical and Geoenvironmental Engineering*, 140(7), p.04014032.
- Maurer, B. W., Green, R. A., Cubrinovski, M., & Bradley, B. A. (2015). Fines-content effects on liquefaction hazard evaluation for infrastructure in Christchurch, New Zealand. *Soil Dynamics and Earthquake Engineering*, 76, 58-68.
- Moss, R., Seed, R., Kayen, R., Stewart, J., Der-Kiureghian, A., & Cetin, K. (2006). CPT-Based probabilistic and deterministic assessment of in situ seismic soil liquefaction potential. *Journal of Geotechnical and Geoenvironmental Engineering*, 132(8).
- NZGD, New Zealand Geotechnical Database (2015). Conditional PGA for Liquefaction Assessment, Map Layer CGD5110 – 30 June 2015, retrieved from <https://www.nzgd.org.nz/>



- NZGD, New Zealand Geotechnical Database (2013). *Liquefaction and Lateral Spreading Observations*, Map Layer CGD0300 - 11 Feb 2013, retrieved from <https://www.nzgd.org.nz/>
- Robertson, P.K. & Wride, C.E., (1998). Evaluating cyclic liquefaction potential using the cone penetration test. *Canadian Geotechnical Journal*, 35(3), pp.442-459.
- Seed, H.B. & Idriss, I.M. (1971). Simplified procedure for evaluating soil liquefaction potential. *Journal of Soil Mechanics & Foundations Div.*
- Taylor, M.L., (2015). The geotechnical characterisation of Christchurch sands for advanced soil modelling. Doctoral Dissertation, University of Canterbury.
- Wotherspoon, L., Orense, R.P., Green, R., Bradley, B., Cox, B. & Wood, C. (2014). Analysis of liquefaction characteristics at Christchurch strong motion stations. *Soil Liquefaction During Recent Large-Scale Earthquakes*, London, UK, pp.33-43.
- Youd, T.L. & Idriss, I.M. (2001). Liquefaction resistance of soils: summary report from the 1996 NCEER and 1998 NCEER/NSF workshops on evaluation of liquefaction resistance of soils. *Journal of geotechnical and geoenvironmental engineering*, 127(4), pp.297-313.